Parallel Study on Surface and Invasive Recordings Across Catheter Ablation Steps of Paroxysmal Atrial Fibrillation

Aikaterini Vraka[1], Fernando Hornero[2], Aurelio Quesada[3], Flavia Ravelli[4], Raúl Alcaraz[5], José J. Rieta[1*]

[1] BioMIT.org, Electronic Engineering Department, Universitat Politecnica de Valencia, Spain; {aivra, jjrieta}@upv.es

[2] Cardiovascular Surgery Department, Hospital Clínico Universitario de Valencia, Valencia, Spain; hornero_fer@gva.es

[3] Cardiology Department, Hospital General Universitario de Valencia, Valencia, Spain; quesada_aur@gva.es

[4] Department of Cellular, Computational and Integrative Biology (CIBIO), University of Trento, Italy; flavia.ravelli@unitn.it

[5] Research Group in Electronic, Biomedical and Telecomm. Eng., Univ. of Castilla-La Mancha, Spain; raul.alcaraz@uclm.es

***Abstract*—Catheter ablation (CA) is the star treatment of atrial fibrillation (AF). However, important issues regarding its procedure have only been superficially explored. While universal CA effect is assessed, the role of right (RPVI) and left pulmonary vein isolation (LPVI) is ignored. Although coronary sinus (CS) is the prevailing CA reference, how CS itself is modified by CA is unknown. This work evaluates the effect of each ablation step on the atrial substrate and CS funtion. Five-minute lead II and bipolar CS recordings of 29 patients undergoing paroxysmal AF CA were acquired before CA, after LPVI and after RPVI (end of CA). Separate lead II and CS analysis was performed. Duration, amplitude, area and slope rate were calculated for each surface and invasive activation, then signal-averaged. Dispersion, morphology variability (MV) and time-domain heart-rate variability (HRV) features were also calculated. Non-parametric tests were recruited to compare each feature among all and in pairs of different ablation steps with Bonferroni correction. Variation of each feature was calculated in percentages. In surface recordings, duration was significantly shortened after LPVI ($\Delta = -13\%$, $p = 0.001$) and HRV showed a trend for attenuation ($\Delta < -25\%$, $p < 0.069$) after RPVI. In CS recordings, HRV showed an increasing trend after LPVI ($\Delta > +73\%$, $p < 0.048$), tending to decrease after RPVI ($\Delta < -33\%$, $p < 0.064$). Higher dispersion in variations was observed in CS than surface recordings. LPVI causes major alterations in atrial substrate, more prominently observed from lead II analysis. Notwithstanding, HRV variations are better illustrated in CS recordings. A combined analysis of both is recommended.**

***Keywords*—Atrial fibrillation; catheter ablation; coronary sinus; substrate assessment; recording catheter.**

I. Introduction

Atrial fibrillation (AF) continues to be the most common cardiac arrhythmia in the western world, while catheter ablation (CA) of pulmonary veins (PVs) remains the cornerstone of AF treatment [1], [2]. In paroxysmal AF patients, P-waves and heart-rate variability (HRV) analysis are commonly recruited in order to predict the outcome of the CA procedure.

P-wave duration, amplitude and area are some of the most highlighted P-wave features, the alteration of which reveals important information on the condition of the atrial substrate [3]–[6]. In general, an attenuation in the aforementioned indices implies a favorable CA outcome, as it is thought to spring from the elimination of fibrotic phenomena, which in turn cause longer and more variable P-waves [5]–[7]. On the other hand, although some degree of HRV is considered normal, HRV reduction after CA of PVs is a temporary aftermath which predicts freedom from AF-recurrence [8].

While analysis of surface recordings is a reliable strategy for the assessment of the CA outcome, it provides generic knowledge on possible atrial substrate alterations. At the same time, how atrial structures are affected due to CA of PVs remains unknown. Coronary sinus (CS) is the most recruited atrial structure as a reference for the AF mapping, actively contributing to the AF initiation or perpetuation [9]–[11]. Therefore, the exploration on alterations of the electrical characteristics of CS due to CA could assist not only into obtaining a deeper knowledge on the effect of CA on the atrial substrate but also to the deconstruction of a key process of CA in order to re-evaluate its validity in substrate modification analysis. The present work analyzes CS recordings of paroxysmal AF patients in sinus rhythm acquired before, during and after CA in order to detect any possible alterations on CS function due to CA. For this purpose P-waves and HRV analysis are used as a reference, undergoing the same analysis on the corresponding surface activations.

II. Materials

Lead II and bipolar CS recordings of 29 paroxysmal AF patients undergoing radiofrequency CA of PVs for the first time formed the database of the study. Recordings were acquired for five minutes before CA, after left PV isolation (LPVI) and

TABLE I

STATISTICAL ANALYSIS FOR P-WAVES. MEDIAN VALUES (INTERQUARTILE RANGE). KRUSKAL-WALLIS ANALYSIS AMONG ALL CHANNELS. MANN-WHITNEY U-TEST WITH BONFERRONI CORRECTION ($\alpha = 0.0167$). STATISTICALLY SIGNIFICANT RESULTS ARE SHOWN IN **BOLD**.

		Median		KW	MWU		
Feature	**Before CA**	**After LPVI**	**After RPVI**		**Bef - LPVI**	**Bef - RPVI**	**LPVI - RPVI**
Duration	120.0 (12.00)	104.0 (13.00)	106.5 (21.00)	**0.0026**	**0.0012**	**0.0094**	0.5580
Amplitude	0.431 (0.303)	0.356 (0.290)	0.374 (0.232)	0.0838	0.0556	0.0967	0.3189
RMS	0.263 (0.179)	0.214 (0.179)	0.230 (0.232)	0.1436	0.1032	0.1500	0.2750
Area	24.63 (12.94)	16.57 (14.62)	20.39 (9.98)	0.1407	0.1032	0.1032	0.4383
S_{20}	0.010 (0.005)	0.011 (0.003)	0.009 (0.005)	0.3358	0.3843	0.6925	0.1329
N$(duration)$	119.5 (57.39)	106.9 (26.04)	101.0 (36.91)	0.1588	0.1412	0.0791	0.7397
N$(atrea)$	26.10 (16.94)	19.40 (14.16)	22.12 (14.01)	0.1443	0.0847	0.1101	0.7160
N(S_{20})	0.010 (0.005)	0.010 (0.008)	0.009 (0.006)	0.8011	0.6925	0.8371	0.5166
MV	0.605 (0.329)	0.753 (0.335)	0.675 (0.467)	0.4760	0.1892	0.6239	0.6464
Dispersion	12.00 (4.000)	11.00 (7.000)	10.00 (4.000)	0.3098	0.2084	0.1761	0.9493
SDNN	94.25 (55.32)	99.91 (71.96)	84.28 (62.10)	0.1359	0.1329	0.8619	0.0598
VARNN	8.8×10^3 (1.07×10^4)	9.9×10^3 (1.77×10^4)	7.1×10^3 (1.21×10^4)	0.1359	0.1329	0.8619	0.0598
RMSSD	95.44 (59.68)	126.79 (95.29)	92.51 (61.73)	0.1359	0.0517	0.9621	0.0689

TABLE II

STATISTICAL ANALYSIS FOR CS LAWS. MEDIAN VALUES (INTERQUARTILE RANGE). KRUSKAL-WALLIS ANALYSIS AMONG ALL CHANNELS. MANN-WHITNEY U-TEST WITH BONFERRONI CORRECTION ($\alpha = 0.0167$). STATISTICALLY SIGNIFICANT RESULTS ARE SHOWN IN **BOLD**.

		Median		KW	MWU		
Feature	**Before CA**	**After LPVI**	**After RPVI**		**Bef - LPVI**	**Bef - RPVI**	**LPVI - RPVI**
Duration	100.5 (14.00)	97.50 (18.00)	90.00 (23.00)	0.1078	0.2411	0.0553	0.2165
Amplitude	1.361 (2.624)	1.382 (1.495)	1.570 (1.462)	0.9416	0.7397	0.9370	0.8371
RMS	0.150 (0.345)	0.151 (0.195)	0.181 (0.218)	0.8471	0.7397	0.9118	0.5583
Area	4.407 (5.175)	3.718 (5.160)	3.985 (4.836)	0.8964	0.6693	0.8371	0.7880
S_{20}	3.8×10^{-4} (0.003)	4.7×10^{-4} (0.001)	5.3×10^{-4} (0.001)	0.9322	0.8868	0.9621	0.6693
N$(duration)$	104.8 (32.83)	102.1 (23.50)	91.25 (33.19)	0.1590	0.6693	0.0598	0.2001
N$(area)$	4.446 (6.861)	3.503 (4.345)	3.832 (4.737)	0.8821	0.6693	0.6925	0.9370
N(S_{20})	4.1×10^{-4} (0.003)	3.9×10^{-4} (0.001)	5.1×10^{-4} (0.001)	0.8364	0.7160	0.8124	0.5798
MV	0.028 (0.048)	0.100 (0.103)	0.067 (0.351)	0.0595	0.0176	0.1134	0.6924
Dispersion	2.500 (3.000)	2.000 (4.000)	2.000 (6.000)	0.6759	0.4613	0.9234	0.4511
SDNN	74.18 (57.56)	96.51 (94.74)	61.75 (73.48)	0.0556	0.0480	0.9118	0.0413
VARNN	5.5×10^3 (7.9×10^3)	9.4×10^3 (2.0×10^4)	3.4×10^3 (1.1×10^4)	0.0556	0.0480	0.9118	0.0413
RMSSD	98.87 (86.99)	127.4 (119.8)	90.40 (74.41)	**0.0489**	0.0257	0.7637	0.0642

after right PV isolation (RPVI) with a sampling frequency of 1 kHz. RPVI matches with the end of CA.

The channel used for the analysis in CS recordings was customly selected for each patient upon inspection as the one with the highest amplitude and least baseline fluctuations. Recordings of the same patient at each ablation point always consisted of the same CS channel, so that the analysis would be reliable and the tracking on CS evolution consistent.

III. METHODS

Preprocessing consisted of denoising and mean removal for both surface and CS recordings [12], [13]. CS recordings were additionally subject to ventricular cancellation [14] if needed. Presence of ectopic beats was less than 4% of total beats for the surface recordings and were corrected via linear interpolation [15]. P-waves and CS local activation waves (LAWs) were detected and delineated [16]–[19].

For each P-wave and CS LAW, duration and amplitude were calculated as described elsewhere [19]. In the present study, amplitude corresponds to peak-to-peak amplitude of the signals. Area was calculated by the integral of the activation's positive amplitude over its duration and slope rate from the following equation:

$$S_{20}^n = \frac{A(t_{20}) - A(t_{onset})}{t_{20} - t_{onset}}, \tag{1}$$

where S_{20}^n is the slope rate of the $n-th$ activation at the 20% of the total duration that it lasts, $A(t_{onset,\ 20})$ is the amplitude at the onset or 20% of the activation, respectively and $t_{onset,\ 20}$ is the sample point corresponding to the $A(t_{onset,\ 20})$.

The following features were calculated obtaining a single value for each lead II and CS recording. Dispersion was the difference between the duration at the $25th$ and $75th$ percentiles. Morphology variability (MV) was the percentage of activations highly correlated ($> 95\%$) with the reference activation. HRV features calculated were: standard deviation of normal-to-normal interval of atrial activa-

tions (SDNN), variance of normal-to-normal interval of atrial activations (VARNN) and root mean square of successive differences between atrial activations (RMSSD).

HR-adjustment was applied for duration, area and slope rate ($\mathbf{N}(duration)$, $\mathbf{N}(area)$ and $\mathbf{N}(S_{20})$, respectively. This normalization was performed for every single activation n by the following equation:

$$\boldsymbol{N}_n = \frac{1000}{R_n - R_{n-1}}, \tag{2}$$

where $n = 1, 2, \cdots, M$ with M- the number of activations of each recording and R_n, R_{n-1} are the R-peaks for the $n-th$ and the $(n-1)-th$ activations, respectively.

Median values were calculated for all features of P-waves and LAWs. Statistical comparison among values at all ablation points for the same feature were performed with Kruskal-Wallis (KW) [20] and comparison between each two ablation points were performed with Mann-Whitney U-test (MWU) [21] with Bonferroni correction, as values did not follow a normal distribution. How features varied after each transition in ablation points (recordings before CA- after LPVI, recordings after LPVI - after RPVI, recordings before CA- after RPVI) was calculated by the variation in percentage.

IV. Results

Tables I and II show the median values of the electrical characteristics of P-waves and LAWs, respectively, before CA, after LPVI and after RPVI. Additionally, the KW comparison among all ablation points as well as the comparison in pairs with MWU with Bonferroni correction are shown. For P-waves, only duration varied statistically among ablation points. Post-hoc analysis revealed that this statistical shortening was observed after LPVI, dropping from 120 ms to 104 ms. Although comparison between ablation points also showed that P-waves after RPVI were significantly shortened with respect to those before CA, this is just a collateral effect of the LPVI. In the opposite case, comparison between P-wave duration of recordings after LPVI and after RPVI would have varied significantly. None of the remaining features varied statistically in P-waves. Nevertheless, some trends were observed for the amplitude after LPVI with respect to that measured before CA as well as for the HRV features when they compared from the recordings between LPVI and RPVI.

Regarding CS LAWs, none of the features calculated at each activation varied significantly after any of the CA steps. Some trends were observed when features across recordings were calculated. MV showed a trend for increase after LPVI, while HRV features showed a trend for increase after LPVI and a trend for attenuation after the end of the procedure. Finally, RMSSD varied significantly among channels. When comparison was performed in pairs of channels, none of the features reached to statistical significance due to Bonferroni correction. However, a trend for RMSSD increasing up to 127.4 after LPVI with respect to 98.87 before the initiation of the procedure, as well as a trend for an overall reduction effect

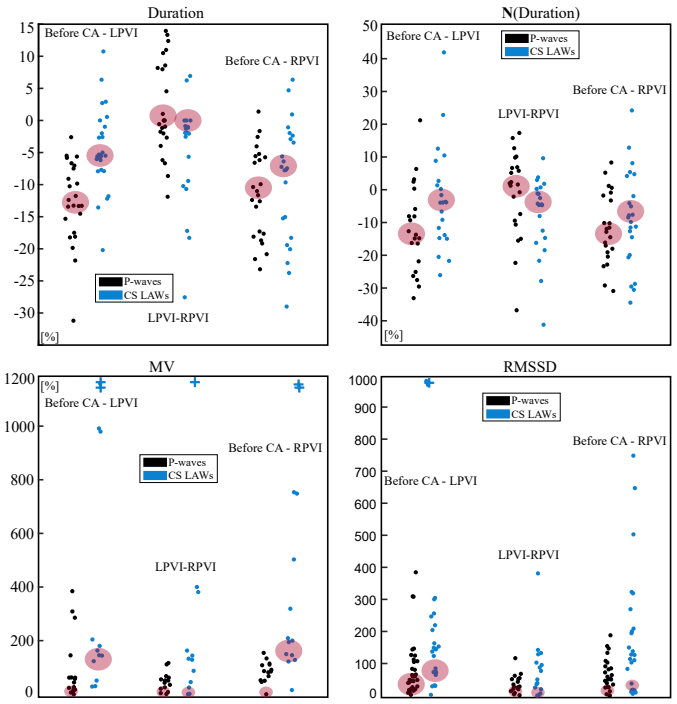

Fig. 1. (a) Scatterplot of variation in percentages for some of the features. For each figure, the first pair corresponds to the transition before CA-after LPVI, the second pair to the LPVI-RPVI transition and the third pair to the transition before-after CA (RPVI). P-waves are shown in black and CS LAWs in blue. Red circles represent the area around the median value of each scatterplot. Small circles represent areas that are below (but close to) zero.

of RMSSD after RPVI (90.40) with respect to the beginning (98.87) of CA were observed.

Finally, Figure 1 shows the scatterplot of variation due to each CA step for duration, $\mathbf{N}$(duration), MV and RMSSD features both in case of P-waves and in case of LAWs. Among all calculated features, these were selected for illustration due to higher variations after each step. Variation in duration and $\mathbf{N}$(duration) was more prominent in P-waves than LAWs after each transition, showing higher negative (shortening) or positive (lengthening) values. For MV and RMSSD, CS LAWs showed higher variations. Additionally, variations in CS LAWs are more dispersed at each feature. This fact is fairly visible in MV and RMSSD, where CS LAWs variations span across a much larger space than the corresponding P-wave values.

V. Discussion

Given the high importance of CS for the CA procedure, knowing how CS function is affected can help to understand deeper the AF mechanisms. For this purpose, bipolar CS as well as surface recordings were recruited and analyzed at each CA step. P-waves analysis revealed a higher relevance with CA procedure than LAWs analysis did, as is shown from the presence of statistical variations in the former which take additionally place to a higher degree than in the case of LAWs analysis. Moreover, P-waves features vary due to CA in a more coherent way than CS LAWs, which showed scattered values. Thus, CA effect is more reliably studied by P-waves analysis.

Considering that CS analysis is limited to local information while P-waves express the effect of CA on the AF substrate in a universal way, the fact that changes are more possibly and to a higher degree observed from P-waves makes sense.

Despite the more visible effect of CA on the electrical characteristics of P-waves, it was CS analysis that revealed more notable variations in HRV and MV after CA. Proximity of CS structure to the tissue directly receiving radiofrequency energy may be the reason for this fact. Even so, a slight variation in P-waves was observed as well.

So far, a statistical shortening of P-waves and HRV attenuation are reported after CA [5], [8]. These results are in line with the results reported in the present study. However, the present study investigated additionally the ablation of which PV part influenced the most the P-wave and CS analysis. This kind of analysis has been rather fruitful, showing that the first part of CA, the LPVI, was crucial for the P-wave shortening. Although HRV was found to be reduced after CA both in P-waves and in LAWs, a temporary incrementation has been observed during CA, attributed to the direct effect of radiofrequency [22]. This effect would have been missed in case that only pre- and postablative recordings were utilized.

VI. Conclusions

Although CS analysis is not indicative of the CA effect on the atrial function, HRV changes are better observed from CS due to its proximity to the tissue under ablation. LPVI is crucial for the alteration of the atrial substrate after CA of AF.

Acknowledgments

Research supported by grants DPI2017–83952–C3 from MINECO/AEI/FEDER UE, SBPLY/17/180501/000411 from JCCLM and AICO/2021/286 from GVA.

References

[1] G. Hindricks, T. Potpara, N. Dagres, E. Arbelo, J. J. Bax *et al.*, "2020 esc guidelines for the diagnosis and management of atrial fibrillation developed in collaboration with the european association of cardio-thoracic surgery (eacts)," *European heart journal*, 2020.

[2] M. Haissaguerre, P. Jaïs, D. C. Shah, A. Takahashi, M. Hocini, G. Quiniou, S. Garrigue, A. Le Mouroux, P. Le Métayer, and J. Clémenty, "Spontaneous initiation of atrial fibrillation by ectopic beats originating in the pulmonary veins," *New England Journal of Medicine*, vol. 339, no. 10, pp. 659–666, 1998.

[3] K. Van Beeumen, R. Houben, R. Tavernier, S. Ketels, and M. Duytschaever, "Changes in p-wave area and p-wave duration after circumferential pulmonary vein isolation." *Europace : European pacing, arrhythmias, and cardiac electrophysiology : journal of the working groups on cardiac pacing, arrhythmias, and cardiac cellular electrophysiology of the European Society of Cardiology*, vol. 12, pp. 798–804, Jun. 2010.

[4] A. Maan, M. Mansour, J. N. Ruskin, and E. K. Heist, "Impact of catheter ablation on p-wave parameters on 12-lead electrocardiogram in patients with atrial fibrillation." *Journal of electrocardiology*, vol. 47, pp. 725–733, 2014.

[5] Q. Chen, S. Mohanty, C. Trivedi, C. Gianni, D. G. Della Rocca, U. Canpolat, J. D. Burkhardt, J. E. Sanchez, P. Hranitzky, G. J. Gallinghouse, A. Al-Ahmad, R. Horton, L. Di Biase, and A. Natale, "Association between prolonged p wave duration and left atrial scarring in patients with paroxysmal atrial fibrillation." *Journal of cardiovascular electrophysiology*, vol. 30, pp. 1811–1818, Oct. 2019.

[6] A. Auricchio, T. Özkartal, F. Salghetti *et al.*, "Short p-wave duration is a marker of higher rate of atrial fibrillation recurrences after pulmonary vein isolation: New insights into the pathophysiological mechanisms through computer simulations." *Journal of the American Heart Association*, vol. 10, p. e018572, Jan. 2021.

[7] R. Alcaraz, A. Martínez, and J. J. Rieta, "The p wave time-frequency variability reflects atrial conduction defects before paroxysmal atrial fibrillation," *Annals of Noninvasive Electrocardiology*, vol. 20, no. 5, pp. 433–445, 2015.

[8] Z. Zhu, W. Wang, Y. Cheng, X. Wang, and J. Sun, "The predictive value of heart rate variability indices tested in early period after radiofrequency catheter ablation for the recurrence of atrial fibrillation." *Journal of cardiovascular electrophysiology*, vol. 31, pp. 1350–1355, Jun. 2020.

[9] M. Antz, K. Otomo, M. Arruda, B. J. Scherlag, J. Pitha, C. Tondo, R. Lazzara, and W. M. Jackman, "Electrical conduction between the right atrium and the left atrium via the musculature of the coronary sinus." *Circulation*, vol. 98, pp. 1790–1795, Oct. 1998.

[10] U. Boles, E. E. Gul, A. Enriquez, N. Starr, S. Haseeb, H. Abdollah, C. Simpson, A. Baranchuk, D. Redfearn, K. Michael *et al.*, "Coronary sinus electrograms may predict new-onset atrial fibrillation after typical atrial flutter radiofrequency ablation (cse-af)," *Journal of atrial fibrillation*, vol. 11, no. 1, 2018.

[11] I. Razeghian-Jahromi, A. Natale, and M. H. Nikoo, "Coronary sinus diverticulum: Importance, function, and treatment." *Pacing and clinical electrophysiology : PACE*, vol. 43, pp. 1582–1587, Dec. 2020.

[12] M. García, M. Martínez-Iniesta, J. Ródenas, J. J. Rieta, and R. Alcaraz, "A novel wavelet-based filtering strategy to remove powerline interference from electrocardiograms with atrial fibrillation." *Physiological measurement*, vol. 39, p. 115006, Nov. 2018.

[13] M. Martínez-Iniesta, J. Ródenas, J. J. Rieta, and R. Alcaraz, "The stationary wavelet transform as an efficient reductor of powerline interference for atrial bipolar electrograms in cardiac electrophysiology." *Physiological measurement*, vol. 40, p. 075003, Jul. 2019.

[14] R. Alcaraz and J. J. Rieta, "Adaptive singular value cancelation of ventricular activity in single-lead atrial fibrillation electrocardiograms." *Physiological measurement*, vol. 29, pp. 1351–1369, Dec. 2008.

[15] A. Martínez, R. Alcaraz, and J. J. Rieta, "Detection and removal of ventricular ectopic beats in atrial fibrillation recordings via principal component analysis." *Annual International Conference of the IEEE Engineering in Medicine and Biology Society. IEEE Engineering in Medicine and Biology Society. Annual International Conference*, vol. 2011, pp. 4693–4696, 2011.

[16] A. Martinez, R. Alcaraz, and J. J. Rieta, "A new method for automatic delineation of ecg fiducial points based on the phasor transform." *Annual International Conference of the IEEE Engineering in Medicine and Biology Society. IEEE Engineering in Medicine and Biology Society. Annual International Conference*, vol. 2010, pp. 4586–4589, 2010.

[17] F. González, R. Alcaraz, and J. J. Rieta, "Electrocardiographic p-wave delineation based on adaptive slope gaussian detection," in *Computing in Cardiology, CinC 2007, Rennes, France, September 24-27, 2017*. www.cinc.org, 2017.

[18] D. I. Osorio, R. Alcaraz, and J. J. Rieta, "A fractionation-based local activation wave detector for atrial electrograms of atrial fibrillation," in *Computing in Cardiology, CinC 2007, Rennes, France, September 24-27, 2017*. www.cinc.org, 2017.

[19] A. Vraka, V. Bertomeu-González, J. Osca, F. Ravelli, R. Alcaraz, and J. J. Rieta, "Study on how catheter ablation affects atrial structures in patients with paroxysmal atrial fibrillation: The case of the coronary sinus," in *2020 International Conference on e-Health and Bioengineering (EHB)*. IEEE, 2020, pp. 1–4.

[20] W. H. Kruskal and W. A. Wallis, "Use of ranks in one-criterion variance analysis," *Journal of the American statistical Association*, vol. 47, no. 260, pp. 583–621, 1952.

[21] H. B. Mann and D. R. Whitney, "On a test of whether one of two random variables is stochastically larger than the other," *The Annals of Mathematical Statistics*, vol. 18, pp. 50–60, 1947.

[22] J. Misek, M. Veternik, I. Tonhajzerova, V. Jakusova, L. Janousek, and J. Jakus, "Radiofrequency electromagnetic field affects heart rate variability in rabbits." *Physiological Research*, vol. 69, no. 4, 2020.